

Circular magnetic x-ray dichroism of 3d impurities in Ni

T. Böske, W. Clemens, C. Carbone, and W. Eberhardt

Institut für Festkörperforschung, Forschungszentrum Jülich D-52425 Jülich, Germany

(Received 15 July 1993)

Circular magnetic x-ray dichroism is studied at the L edges of the 3d transition metal series (Cr, Mn, Fe, and Co) as impurities in a nickel host, using partial fluorescence yield to monitor the absorption. While the latter 3d metals Mn, Fe, and Co couple ferromagnetically to the Ni host, Cr is found to couple antiferromagnetically. Using a sum rule derived within an atomic description we obtain values of the spin magnetic moment of the impurities, which are in good agreement with calculations.

I. INTRODUCTION

Experimental evidence for the interaction between light and magnetic fields has existed since the 19th century. These phenomena include Faraday rotation and the magneto-optical Kerr effect (MOKE). All these effects were observed in the optical region of the electromagnetic spectrum. Only recently, stimulated through the advent of synchrotron light sources with the possibility to obtain polarized light of high intensity over a broad spectral range, experimentalists and theoreticians started to study magneto-optical effects in magnetically ordered substances in the x-ray energy regime. This photon energy range covers optically induced core to valence transitions in rare-earth and transition metals. The magneto-optical effects studied include magnetic x-ray dichroism (MXD),¹⁻⁵ x-ray Faraday rotation,⁶ and magnetic x-ray scattering.⁷

Dichroism in general may be defined as a polarization-dependent absorption coefficient. MXD is the magnetic field induced polarization dependency of the absorption coefficient in the x-ray energy regime. Depending on the character of the polarization, one discriminates between linear (LMXD) and circular magnetic x-ray dichroism (CMXD). The first theoretical study of CMXD was undertaken by Erskine and Stern¹ in the $M_{2,3}$ absorption spectra of ferromagnetic nickel, showing the close relationship between CMXD and MOKE. The most fundamental property of CMXD was predicted in this paper, namely, its possibility to obtain the spin polarization of the unoccupied d electronic states. The first experimental evidence of MXD has been reported by van der Laan *et al.*² for magnetically ordered Tb at the M_5 edge; the first experimental study of CMXD has been performed by Schütz *et al.*³ at the Fe K edge. The transition metal L edges have been studied by Chen and co-workers recently,^{5,8} where a strong CMXD is observed in the prominent $2p \rightarrow 3d$ core to valence transition.

It is frequently assumed that MXD can be used to determine local partial magnetic moments of magnetically ordered materials.^{3,4} The terms local and partial in this context mean that due to the localized character of the core hole and due to the dipole selection rules, one can

obtain atom and shell specific values for the magnetization. Calculations for rare-earth metals show indeed that with CMXD it is possible to obtain magnitude and direction of local partial magnetic moments, while LMXD is sensitive to the magnitude of the magnetization but not to the direction, making the former method useful for ferro- and ferrimagnetic materials and the latter additionally for antiferromagnetic materials.⁴

MXD for the transition metal L edges has successfully been described within the Anderson impurity model taking configuration interaction into account.^{9,10} Within an atomic approach, it is possible to calculate the orbital as well as the spin contribution to the magnetic moment, whereas simple one particle band approaches in an itinerant model only concentrate on the spin.^{1,3} Although the orbital moment for transition metals is very small compared to the spin moment, it determines important macroscopic effects, like the magnetocrystalline anisotropy and the easy axis of magnetization.¹¹ In multilayer systems, in particular, orbital moments can be enhanced strongly compared to pure metals, and it is a matter of discussion whether or not local spin moments can be obtained with CMXD for multilayers exhibiting large orbital moments.¹² The determination of orbital magnetic moments using fully relativistic band structure calculations has also been carried out.¹³ These calculations have the appealing property to be fully parameter free, and are applied to systems described by itinerant magnetism.¹⁴

To obtain local partial magnetic moments, two sum rules have been stated in the atomic model, which relate the dichroic signal over the spin-orbit split edges to ground state expectation values for the orbital¹⁵ and the spin momentum¹⁶ per hole. The importance of sum rules has been established in spectroscopy, because important information on ground state properties may be obtained despite the rather restricted information on the distribution of the spectral intensity over the range in question.¹⁷ Whereas the sum rule for the orbital momentum has been verified experimentally,^{12,15} we would like to demonstrate in this article that applying the spin sum rule to the experimental CMXD spectra of 3d impurities in Ni yields good results in accordance with theoretical calculations on impurity spin moments.

To do this, we used a thin Co film epitaxially grown on a Cu single crystal to calibrate the degree of circular polarization. Using this value, we calculate the local impurity spin moments with the help of the spin sum rule. It is important to note, however, that we are able to locate the transition from antiferromagnetic to ferromagnetic coupling of the impurity spin to the host independent of the application of sum rules, since CMXD is sensitive to the direction of the magnetic moment, as already recognized by Erskine and Stern.¹

II. EXPERIMENT

The experiments were performed at the SX700-III beam line of the BESSY synchrotron facility in Berlin. This beam line has recently been equipped with two moveable plane premirrors to provide elliptically polarized synchrotron radiation above and below the plane of the storage ring, extending the use from originally linearly polarized to circularly polarized light.¹⁸ Our measurements were all taken with σ^+ radiation $+0.3$ mrad off plane, and it is expected from calculations that the degree of circular polarization should be nearly constant and exceeds 50% in the energy region of the $3d$ transition metal L edges. The precise degree of circular polarization is not known, but from Fe L core level photoemission—using photons of about 850 eV—a polarization of $70 \pm 10\%$ was deduced.¹⁹ However, we must stress that the polarization depends crucially on the exact beam position, the mirror setting, and the aperture, which selects the radiation of interest; therefore deviations from the above mentioned value are not unexpected.

Our samples were thin nickel foils with an amount of 2% of the impurities Cr, Mn, Fe, and Co, which were produced by melting in a high purity argon atmosphere.²⁰ The concentrations of transition metal impurities and the preparation procedure were chosen carefully in order to obtain a homogeneous solution without forming precipitates. The lattice distortion due to the impurities leads to maximal 0.9% (in Ni-Mn) increased nearest Ni neighbor distance around the impurity atom relative to pure Ni, whereas the second neighbor distance is unchanged.²⁰ The coordination number for the impurity site turns out to be 12.1 ± 1.0 , very close to the value for a fcc crystal. We conclude, therefore, that the crystalline structure of the examined $3d$ impurities in Ni is essentially fcc with only very small deviation from the host structure.

The foils were magnetized *in situ* using a SmCo₅ permanent magnet with a magnetic field strength of about 0.2 T at the sample position. The magnet could be rotated to change the direction of the magnetization without changing the sample position or switching to the complementary polarization in selecting other mirror and aperture settings, which could influence the degree of circular polarization and the resolution. Because of the diluted samples, high photon flux was required to obtain reasonable data acquisition times. Therefore the spectra were recorded with a 50- μm slit, the resulting resolution is about 1.5 eV at the Mn L edges and 2.5 eV for the Co L edges.

The absorption signal in our experiment was monitored

in partial fluorescence-yield (FY) mode. This detection mode is not influenced by the presence of an external magnetic field. It is ideally suited for diluted samples, because the signal is directly proportional to the absorption coefficient in question and the signal-to-noise ratio is higher than in electron-yield.²¹ The outgoing fluorescent radiation, which is produced after annihilation of a core hole in the $L_{2,3}$ shell, is detected with a high purity germanium crystal detector with a resolution of better than 100 eV, sufficient to discriminate against nickel radiation or radiation from contaminations on the surface, like carbon or oxygen.

Recently, the polarization dependence of the L emission spectra of magnetized iron has been studied,²² showing a dichroic effect in soft x-ray emission in the order of 1%. Such effects do not influence our spectra, because they only change the absolute FY intensity, which scales out due to the normalization procedure. Dynamic effects in polarization-dependent L emission of pure $3d$ metal ferromagnets using monochromatic synchrotron radiation have been observed very recently.²³ In these experiments it is important to discriminate between CMXD in absorption and CMXD in emission, since absolute intensity differences are—at least partially—due to different absorption cross sections for σ^+ and σ^- radiation, which is the topic of this article. A conclusive demonstration that the observed intensity differences are solely due to CMXD in the emission process is lacking up to now. One must be aware, although, that *energy-dependent* CMXD in emission in principle does influence the FY.

III. RESULTS AND DISCUSSION

This section contains the experimental results and some theoretical background. In the first part, we show CMXD measurements of a thin Co film, grown on Cu(100). We take this system to calibrate the degree of circular polarization using the spin sum rule explained in the following. The second part is dedicated to the $3d$ impurities in Ni.

Magnetic dichroism is dominated by angular momentum selection rules, making an atomic description a reasonable first step approach. This model can be extended to any crystal symmetry including ligand-field interactions.²⁴ In absorption at the L edges of transition metals we are investigating the $2p^6 3d^n \rightarrow 2p^5 3d^{n+1}$ excitation into the empty $3d$ states. The symmetry of the initial and the final states can be described within the LS -coupling approximation, which results in different JLS levels, each $(2J + 1)$ -fold degenerate. In the presence of a magnetic field—due to, e.g., interatomic exchange interaction—the J levels split into $2J + 1$ sublevels with different M in the well known way. The possible transitions $(JM) \rightarrow (J'M')$ are governed by the dipole selection rules, which for circularly polarized light are reading $J' - J = 0, \pm 1$ and $M' - M = \pm 1$ (for photons with positive-negative helicity). The distribution of the line strength of the transition $(J, M) \rightarrow (J', M')$ from one M to different M' values is determined by the angular- and spin symmetry of the wave functions.

For the transition metal L edges, only excitations into the spin-orbit split $2p_{\frac{3}{2}} d^{n+1}$ and $2p_{\frac{1}{2}} d^{n+1}$ states can be resolved, which are corresponding to the L_2 and L_3 absorption edges respectively.²⁴ In rare-earth metals spectral features due to different final state J' values can be resolved,^{2,4} and the local magnetic moments can be obtained by multiplet analysis. This is not the case for the 3d metals, where multiplets of the initial $3d^n$ and final $2p^5 3d^{n+1}$ configuration can only partially be resolved. Dichroism is present here in different intensities in the L absorption edges as a result of the interplay between different occupation numbers of the magnetically split sublevels and the dipole selection rules for circularly polarized light.²⁴ A relation between the integrated absorption intensity at the L_3 and L_2 edges and the po-

larization of the exciting light may reveal information on local magnetic moments.

By symmetry arguments it is equivalent to either keep the magnetization direction and switch between σ^+ and σ^- light, or to fix the polarization of the light while changing the magnetization direction. It has been shown that the difference of the integrated absorption intensity for circularly polarized light parallel (I^+) and antiparallel (I^-) to the magnetization direction is proportional to the ground state expectation value of the orbital momentum $\langle L_z \rangle$ per hole.¹⁵ Recently a new CMXD sum rule has been derived by Carra *et al.*,¹⁶ which relates the integral of the dichroic signal over a single partner of a spin-orbit split edge to the ground state expectation value of $\langle S_z \rangle$.

These sum rules state in detail¹⁶

$$\frac{\int_{L_3+L_2} dE (I^+ - I^-)}{\int_{L_3+L_2} dE (I^+ + I^- + I^0)} = \frac{1}{2} \frac{\ell(\ell+1) + 2 - c(c+1)}{\ell(\ell+1)(4\ell+2-n)} \langle L_z \rangle, \quad (1)$$

$$\frac{\int_{L_3} dE (I^+ - I^-) - \left(\frac{c+1}{c}\right) \int_{L_2} dE (I^+ - I^-)}{\int_{L_3+L_2} dE (I^+ + I^- + I^0)} = \frac{\ell(\ell+1) - 2 - c(c+1)}{3c(4\ell+2-n)} \langle S_z \rangle + \frac{\ell(\ell+1)\{\ell(\ell+1) + 2c(c+1) + 4\} - 3(c-1)^2(c+2)^2}{6\ell c(\ell+1)(4\ell+2-n)} \langle T_z \rangle. \quad (2)$$

$4\ell+2-n$ is the number of 3d holes in the valence band, and ℓ and c are denoting the angular momenta of the valence electron and the core hole (in our case $\ell=2$ and $c=1$). $\langle T_z \rangle$ is the expectation value of the magnetic dipole operator and is a measure of magnetic anisotropy due to spin-orbit interaction or crystal field effects.²⁵ Spin-spin interaction vanishes in first order in cubic or higher symmetries, and a contribution to $\langle T_z \rangle$ can be obtained in higher order only with spin-orbit interaction. The energy integration extends over the L_3 and/or over the L_2 edges as indicated. I^+ denotes the absorption with the magnetization parallel, I^- antiparallel, and I^0 perpendicular to the photon angular momentum vector. The isotropic absorption is given by $I^{\text{is}} = \frac{1}{3}(I^+ + I^- + I^0)$. In our analysis we assumed that $I^0 = \frac{1}{2}(I^+ + I^-)$.

The advantage of the sum rules is clearly at hand: To derive the expressions above, only angular and spin symmetries have to be considered. The details of the distribution of the spectral intensity across different transitions within one multiplet do not enter. Further, one only has to know the occupation number of the valence band in question. One has to keep in mind although that, whereas Eq. (1) is correct for arbitrary symmetry, Eq. (2) gives spin moments in fairly good approximation only for systems with cubic or higher symmetries.¹⁶ In our context, concerning impurities in a fcc lattice, the sum rules are nevertheless a great advantage to previous models, where one has to know the total density of unoccupied states as a function of energy to obtain local magnetic moments.²⁶

With $\langle S_z \rangle$ we calculate the local spin magnetic moment according to

$$\mu_S = \frac{1}{P_c} g_S \mu_B \langle S_z \rangle, \quad (3)$$

where g_S is the gyromagnetic factor for the electronic spin moment, which is ≈ -2.0 . The factor P_c takes incomplete circular polarization into account. In deriving this expression, we neglected the magnetic dipole interaction. Similarly, the local orbital magnetic moment can be calculated to be

$$\mu_L = \frac{1}{P_c} g_L \mu_B \langle L_z \rangle, \quad (4)$$

with $g_L = -1$. It is important to note that these sum rules are shell selective, which is induced via dipole transitions into final states involving core holes of definite symmetry LS . The moments obtained with these sum rules are the local moments for electrons with d character, in so far as the dipole approximation for the electronic transition holds.

A. Thin Co film

A 40-Å Co film was grown on the (100) surface of a clean and well ordered Cu single crystal under UHV conditions by evaporating high purity Co. Cleanliness and crystalline structure were checked by standard methods. Details of the preparation procedure can be found elsewhere.²⁷ After the evaporation, a capping layer of 150 Å Cu was put *in situ* on top to avoid surface contamination of the Co layer. Co grows epitaxially in a layer-by-layer mode on Cu(100); the film is ferromagnetic at room

temperature with in-plane (110) magnetization axis. The thickness of the Co layer was chosen to match the following two requirements: First, the Co film should exhibit bulk electronic properties, and second, the film should not be too thick to cause distortions due to so-called self absorption effects in the spectra.²¹

The measurements were performed under identical conditions as for the impurities, save for a better resolution of 1.5 eV due to a 20- μm slit. In the center panel of Fig. 1 we show the absorption of body-centered tetragonal (bct) Co for σ^+ circularly polarized light with magnetization parallel and antiparallel to the photon angular momentum. The spectra were normalized to the incident

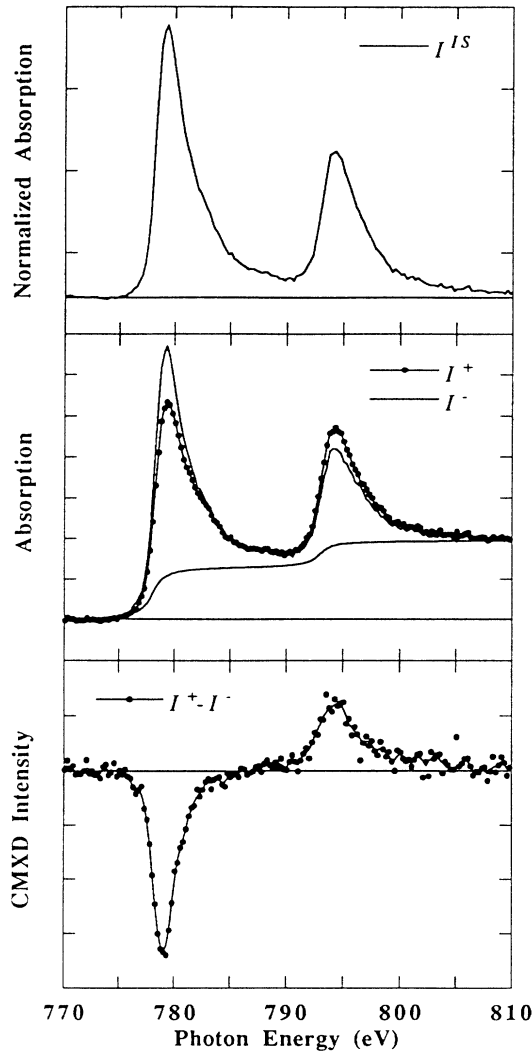


FIG. 1: Fluorescence-yield x-ray appearance near-edge structure (XANES) spectra of the $L_{2,3}$ edges of bct Co on Cu (100) with σ^+ circularly polarized light. Center panel: absorption spectra for magnetization parallel (I^+ dotted line) and antiparallel (I^- plain line) to the photon angular momentum. Also shown is the step function. Top panel shows the resulting isotropic white line intensity (I^{is}) obtained from the spectra after subtracting the step function. Bottom panel shows the difference spectrum between absorption with parallel and antiparallel magnetization ($I^+ - I^-$).

photon flux, determined with a gold mesh, and rescaled to a constant height far above the L edges. We subtracted the steplike function shown in the center panel to account for the continuum background for each edge. The height of the steps was kept to the statistical ratio of 2 : 1 for the $L_3 : L_2$ step; the step position and width were determined approximately from the inflection point at the rising edge of the spectra. The resulting isotropic intensity (I^{is}) and the difference spectra ($I^+ - I^-$) are shown in the upper and lower panel of Fig. 1.

The crystalline structure of Co on Cu(100) is not exactly cubic, due to the lattice mismatch between Cu and Co. This leads to a bct Co lattice with $c/a = 0.95$, which means only a small deviation from cubic symmetry.²⁸ By applying Eq. (3) we neglected the magnetic dipole interaction, and as we have discussed above, this is a good approximation only for systems with at least cubic symmetry. We argue that the deviation of the bct from a fcc lattice results in a small contribution to the expectation value of the magnetic dipole operator $\langle T_z \rangle$, and we estimate it to be less than 5% of $\langle S_z \rangle$, by taking values for the calculated dipole-dipole interaction as a function of c/a for Co.²⁹ We obtain a degree of circular polarization P_c of 48%, taking the local partial magnetic moment of d character of bct Co to be $1.64\mu_B$ and the $3d$ occupation number n to be 7.13.²⁸ Uncertainties in the determination of the step function and the normalization of the spectra relative to each other can affect the degree of polarization seriously, and we estimate the errors to be in order of 20% of the above obtained value for P_c . We will take this value for the circular polarization to calculate the local magnetic spin moments of the impurities in the following section.

The ratio $\langle L_z \rangle / \langle S_z \rangle$ is independent of the degree of circular polarization and the $3d$ occupation number n , as can be seen from the sum rules [Eq. (1) and (2)], and it can be obtained directly from the CMXD spectra. Using the appropriate values for c and ℓ this ratio is given by

$$\frac{\langle L_z \rangle}{\langle S_z \rangle} = \frac{4}{3} \frac{\int_{L_3+L_2} dE (I^+ - I^-)}{\int_{L_3} dE (I^+ - I^-) - 2 \int_{L_2} dE (I^+ - I^-)}, \quad (5)$$

again neglecting $\langle T_z \rangle$.¹⁶ The total magnetic moment is given by $\mu_{\text{tot}} = -\mu_B(\langle L_z \rangle + 2\langle S_z \rangle)$, and the ratio $\mu_{\text{spin}}/\mu_{\text{tot}}$ is independent of the degree of circular polarization P_c and of the number of unoccupied states in the $3d$ band n too. In Table I we show the results for $\langle L_z \rangle / \langle S_z \rangle$ and $\mu_{\text{spin}}/\mu_{\text{tot}}$ for the bct Co film, and calculations on pure fcc Co metal,¹¹ demonstrating, that the atomlike picture used to derive the sum rules is appropriate to describe the CMXD spectra.

TABLE I. Ratio of orbital to spin ground state expectation values and spin to total magnetic moments of the bct Co film, compared to theoretical values for pure fcc Co.

	$\langle L_z \rangle / \langle S_z \rangle$	$\mu_{\text{spin}} / \mu_{\text{tot}}$
This work: bct Co film	0.16 ± 0.03	0.925 ± 0.06
fcc Co ^a	0.15	0.93

^aFrom Ref. 11.

B. 3d impurities in Ni

In a ferromagnetic host, the magnetic moment of an impurity can couple either parallel or antiparallel to the host moment. One direction is energetically favored, because of the the break of the symmetry of the exchange field by the spontaneous magnetization of the host. The magnitude of the impurity moment is influenced by the hybridization with the host. Calculations of the local spin moments of 3d impurities in nickel^{30,31} show that the spin of the early transition metals couples antiferromagnetically to the spin of the Ni host, whereas the late transition metals couple ferromagnetically. Theory predicts a change of the sign of the coupling in the middle of the 3d series, and favors the transition from antiparallel to parallel coupling to be between Cr and Mn.³¹ This is similar to the case of 5d impurities in Fe, where the transition occurs later in the series, as has been studied experimentally with CMXD.²⁶

Experiments on 3d impurities in Ni were performed so far with neutron scattering by several groups (see Ref. 30 for a collection of data). It is established that the later 3d metals (Mn, Fe, and Co) couple ferromagnetically; the earlier couple antiferromagnetically. But for Cr the experimental data from neutron scattering are ambivalent: One cannot definitely state whether Cr couples ferro- or antiferromagnetically with respect to the nickel host. It has to be pointed out, also, that for Cr the calculations are very sensitive to the exact form of the chosen potentials and that local lattice relaxations are not included,

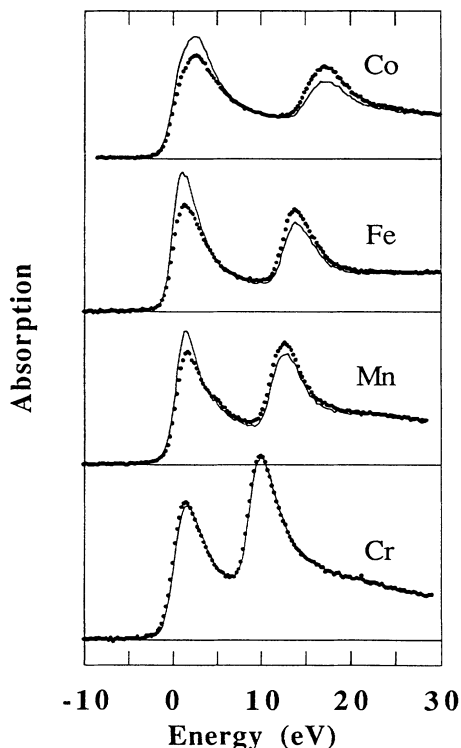


FIG. 2. Fluorescence-yield XANES spectra of the $L_{2,3}$ edges of Cr, Mn, Fe, and Co impurities in nickel with circularly polarized light of positive helicity (σ^+). Dotted line (plain line) shows the absorption with the magnetization (anti)parallel to the photon angular momentum I^+ (I^-).

so that the magnitude of the calculated spin moment is subject to large uncertainties.

In Fig. 2 the $L_{2,3}$ absorption spectra at room temperature of Cr, Mn, Fe, and Co impurities in Ni are shown, taken with the sample magnetization parallel (I^+) and antiparallel (I^-) to the photon angular momentum. Figure 3 shows the difference $I^+ - I^-$, which is the CMXD signal. The spectra were normalized as mentioned above in Sec. III A; the energy scale was set to the first inflection point of the L_3 edges. The following observations can be made.

(1) The CMXD signal at the L_3 edge is negative for Mn, Fe, and Co in Ni; it is much smaller and positive for Ni-Cr.

(2) The corresponding CMXD signal at the L_2 edge has reversed sign and lower intensity.

The lower integrated intensity of the L_2 in comparison to the L_3 edge in the CMXD spectra reflects the fact that the contribution of orbital moments to the total magnetic moments has to be taken into account,^{9,10} as may be seen directly from the orbital sum rule in Eq. (1). The CMXD signal of Cr is the smallest of the examined 3d metals, which is caused by a comparable small magnetic moment. The vanishingly small CMXD signal at the L_2 edge reflects this—together with incomplete circular polarization—rather than a large orbital moment for Cr.

CMXD yields the orientation of the impurity spin to the quantization axis, which is just given by the magnetization direction of the nickel host. If $I^+ - I^-$ at the L_3 edge is positive (negative), the local impurity moment is oriented antiparallel (parallel) to the host moment.¹

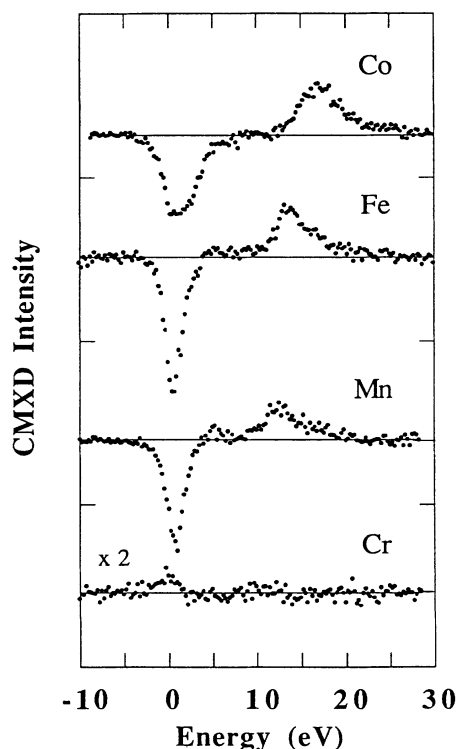


FIG. 3. Difference spectra ($I^+ - I^-$) between parallel and antiparallel magnetization of the CMXD spectra in Fig. 2. The difference spectrum of Cr has been multiplied by 2.

The reverse holds for the L_2 edge. Therefore we have established that the transition from antiferromagnetic to ferromagnetic coupling in the $3d$ series in Ni takes place between Cr and Mn.

For a quantitative analysis of the spin moments we should discuss some experimental aspects in detail.

(1) The measurements were done at room temperature; therefore the saturation magnetization of the Ni foil is reduced, but it is still more than 90% of the ground state value. Temperature effects for the impurities are more important, as has been shown in neutron scattering measurements (see Ref. 32 for Ni-Mn). While for Fe and Co magnetic moments are nearly temperature independent, the moments of Cr and Mn are strongly influenced.

(2) In a fcc crystal (like Ni) the coordination number is 12; therefore the probability to have two impurity atoms as nearest neighbors in a homogeneous distribution of 2 at. % is about 25%. Consequently, effects due to impurity-impurity interactions have to be taken into account. Calculations of the impurity-impurity interaction in Ni show that the impurity moments couple ferromagnetically to each other.³³ The magnetic moments are reduced due to impurity pairing by $0.1\mu_B$, $0.06\mu_B$, and $0.02\mu_B$ for Mn, Fe, and Co respectively. From neutron scattering experiments it can be deduced, that the magnetic moments of Cr and Mn decrease with increasing concentration, while the Fe and Co moments are nearly independent of the concentration.

This discussion shows that the magnetic moments of Co impurities are nearly independent of temperature and concentration, while the ones for Cr and Mn could be considerably smaller than the ground state values of a dilute system.

In Fig. 4 we show the local magnetic moment, obtained with the spin sum rule [Eq. (2)] out of our CMXD spectra using Eq. (3), compared to the calculated values by Blügel *et al.*³¹ We have taken calculated occupation numbers n for the $3d$ valence band by Zeller,³⁰ and used the value for P_c determined in Sec. III A. Thus the magnetic spin moments (in units of μ_B) we obtain from our data are $\mu_{Cr} = -0.16 \pm 0.10$, $\mu_{Mn} = 2.25 \pm 0.35$, $\mu_{Fe} = 2.58 \pm 0.28$, $\mu_{Co} = 1.74 \pm 0.21$. As can be seen in Fig. 4, the overall shape of the curve is in accordance with the calculated one. The magnetic moments of Mn and Cr differ from the calculations as can be expected from our discussion above. For Mn this difference is in the range of temperature and concentrational variations; for Cr, on the other hand, the experimental value is much smaller than the calculated one, giving reason to assume that temperature variations and the concentration of the Cr impurity have a large impact on the local magnetic moment.

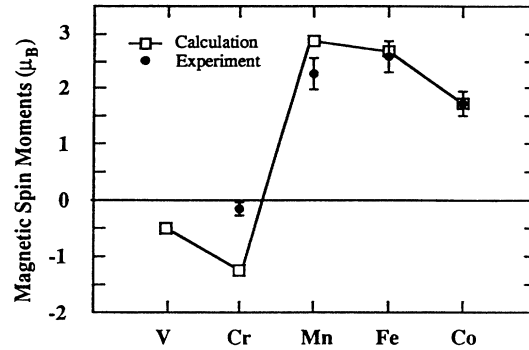


FIG. 4. Local magnetic spin moments of $3d$ impurities in Ni. Open squares: calculation by Blügel *et al.* (Ref. 31). The line is drawn to guide the eye only. Solid circles: this work (see text for details).

IV. CONCLUSION

In conclusion we have demonstrated that fluorescence detection of CMXD can be used efficiently to study local magnetism of diluted systems—as in $3d$ impurities in Ni—and buried layers—as in Cu/Co/Cu (100). We apply a recently derived sum rule to determine the degree of circular polarization and to evaluate the local partial spin moments of $3d$ impurities in Ni. We compare the results with calculated magnetic moments and neutron scattering data, and demonstrate that CMXD is under certain conditions capable of separating spin and orbital contributions to the total magnetic moment. One result of this work, however, can be stated without the application of sum rules and their approximations: Our experiment shows that the transition from antiferromagnetic to ferromagnetic coupling of the spin of $3d$ impurities in Ni takes place between Cr and Mn, as predicted by calculations.

ACKNOWLEDGMENTS

The experiments were performed at the BESSY storage ring in Berlin. We would like to thank the BESSY staff for support. Special thanks to M. Willmann (BESSY), A. Knop (Sietec), and E. Navas (FU Berlin). We thank B. Lengeler for providing the impurity samples, T. Kachel (BESSY) for help in preparing the Co film, S. Blügel and R. Zeller for fruitful discussions. Also, we would like to thank C. Vettier and P. Carra (ESRF) and L.-C. Duda (Uppsala University) for providing valuable information prior to publication.

¹ J. L. Erskine and E. A. Stern, Phys. Rev. B **12**, 5016 (1975).

² G. van der Laan, B. T. Thole, G. A. Sawatzky, J. B. Goedkoop, J. C. Fuggle, J. M. Esteva, R. Karnatak, J. P. Remeika, and H. A. Dabkowska, Phys. Rev. B **34**, 6529 (1986).

³ G. Schütz, W. Wagner, W. Wilhelm, P. Kienle, R. Zeller, R. Frahm, and G. Materlik, Phys. Rev. Lett. **58**, 737

(1987).

⁴ J. B. Goedkoop, B. T. Thole, G. van der Laan, G. A. Sawatzky, F. M. F. de Groot, and J. C. Fuggle, Phys. Rev. B **37**, 2086 (1988).

⁵ C. T. Chen, F. Sette, Y. Ma, and S. Modesti, Phys. Rev. B **42**, 7262 (1990).

⁶ D. P. Siddons, M. Hart, Y. Amemiya, and J. B. Hastings, Phys. Rev. Lett. **64**, 1967 (1990).

- ⁷ C. Vettier, D. B. McWhan, E. M. Gyorgy, J. Kwo, B. M. Buntschuh, and B. W. Batterman, *Phys. Rev. Lett.* **56**, 757 (1986).
- ⁸ F. Sette, C. T. Chen, Y. Ma, S. Modesti, and N. V. Smith, in *X-Ray Absorption Fine Structure*, edited by S. S. Hasnain (Ellis Horwood, New York, 1991).
- ⁹ T. Jo and G. A. Sawatzky, *Phys. Rev. B* **43**, 8771 (1991).
- ¹⁰ G. van der Laan and B. T. Thole, *J. Phys. Condens. Matter* **4**, 4181 (1992).
- ¹¹ O. Eriksson, B. Johansson, R. C. Albers, A. M. Boring, and M. S. S. Brooks, *Phys. Rev. B* **42**, 2707 (1990).
- ¹² Y. Wu, J. Stöhr, B. D. Hermsmeier, M. G. Samant, and D. Weller, *Phys. Rev. Lett.* **69**, 2307 (1992).
- ¹³ H. Ebert, R. Zeller, B. Drittler, and P. H. Dederichs, *J. Appl. Phys.* **67**, 4576 (1990).
- ¹⁴ S. Stähler, G. Schütz, and H. Ebert, *Phys. Rev. B* **47**, 818 (1993).
- ¹⁵ B. T. Thole, P. Carra, F. Sette, and G. van der Laan, *Phys. Rev. Lett.* **68**, 1943 (1992).
- ¹⁶ P. Carra, B. T. Thole, M. Altarelli, and X. Wang, *Phys. Rev. Lett.* **70**, 694 (1993).
- ¹⁷ H. A. Bethe and E. E. Salpeter, *Quantum Mechanics of One- and Two- Electron Atoms* (Springer Verlag, Berlin, 1957).
- ¹⁸ M. Willmann, H. Petersen, F. Schäfers, M. Mast, B. R. Müller, and W. Gudat (unpublished).
- ¹⁹ L. Baumgarten, C. M. Schneider, H. Petersen, F. Schäfers, and J. Kirschner, *Phys. Rev. Lett.* **65**, 492 (1990).
- ²⁰ U. Scheuer and B. Lengeler, *Phys. Rev. B* **44**, 9883 (1991).
- ²¹ S. Eisebitt, T. Böske, J.-E. Rubensson, and W. Eberhardt, *Phys. Rev. B* **47**, 14 103 (1993).
- ²² C. F. Hague, J.-M. Mariot, P. Strange, P. J. Durham, and B. L. Gyorffy, *Phys. Rev. B* **48**, 3560 (1993).
- ²³ L. -C. Duda and N. Wassdahl (private communication).
- ²⁴ G. van der Laan and B. T. Thole, *Phys. Rev. B* **43**, 13 401 (1991).
- ²⁵ J. Kanamori, in *Magnetism*, Vol. 1, edited by G. T. Rado and H. Suhl (Academic Press, New York, 1963).
- ²⁶ R. Wienke, G. Schütz, and H. Ebert, *J. Appl. Phys.* **69**, 6147 (1991).
- ²⁷ W. Clemens, T. Kachel, O. Rader, E. Vescovo, S. Blügel, C. Carbone, and W. Eberhardt, *Solid State Commun.* **81**, 739 (1992).
- ²⁸ W. Clemens, H. Kino, and S. Blügel (unpublished).
- ²⁹ G. H. O. Daalderop, P. J. Kelly, and M. F. H. Schuurmans, *Phys. Rev. B* **41**, 11 919 (1990).
- ³⁰ R. Zeller, *J. Phys. F* **17**, 2123 (1987).
- ³¹ S. Blügel, H. Akai, R. Zeller, and P. H. Dederichs, *Phys. Rev. B* **35**, 3271 (1987).
- ³² J. W. Cable and H. R. Child, *Phys. Rev. B* **10**, 4607 (1974).
- ³³ T. Hoshino, W. Schweika, R. Zeller, and P. H. Dederichs, *Phys. Rev. B* **47**, 5106 (1993).